PHYSICAL REVIEW D **88,** 076005 (2013)

Anatomy of relativistic pion loop corrections to the electromagnetic nucleon coupling

Chueng-Ryong Ji,[1] W. Melnitchouk,[2] and A. W. Thomas[3]

[1]*Department of Physics, North Carolina State University, Raleigh, North Carolina 27692, USA*
[2]*Jefferson Lab, 12000 Jefferson Avenue, Newport News, Virginia 23606, USA*
[3]*CSSM and CoEPP, School of Chemistry and Physics, University of Adelaide, Adelaide SA 5005, Australia*

(Received 26 June 2013; published 9 October 2013)

We present a relativistic formulation of pion loop corrections to the coupling of photons with nucleons on the light front. Vertex and wave function renormalization constants are computed to lowest order in the pion field, including their nonanalytic behavior in the chiral limit, and studied numerically as a function of the ultraviolet cutoff. Particular care is taken to explicitly verify gauge invariance and Ward-Takahashi identity constraints to all orders in the m_π expansion. The results are used to compute the chiral corrections to matrix elements of local operators, related to moments of deep-inelastic structure functions. Finally, comparison of results for pseudovector and pseudoscalar coupling allows the resolution of a longstanding puzzle in the computation of pion cloud corrections to structure function moments.

DOI: 10.1103/PhysRevD.88.076005 PACS numbers: 11.30.Rd, 11.10.Gh, 12.39.Fe, 13.60.Hb

I. INTRODUCTION

The importance of chiral symmetry in hadron physics has been understood for more than 50 years. As an explicit Lagrangian representation of the approximate chiral symmetry that had been recognized in low-energy pion-nucleon interactions, Gell-Mann and Levy [1] constructed the extremely successful linear sigma model. In that model the pion couples to the nucleon through pseudoscalar coupling, while an additional scalar (σ) field is also coupled linearly. At a more formal level, Gell-Mann [2] proposed SU(2) $\times$ SU(2) as an exact algebra for the charges associated with the Hamiltonian governing the strong interaction, even though chiral symmetry was not an exact symmetry of that Hamiltonian.

On the basis of current algebra one can show very generally that the amplitude for pion scattering or production must vanish as the four-momentum of the pion vanishes [3,4]. Within the linear sigma model, this important result for low-energy pion-nucleon scattering, for example, is only possible through a subtle cancellation of two large contributions, the first involving pion emission and absorption through the pseudoscalar (PS) coupling, and the second involving σ exchange in the t channel. Keeping track of the necessary cancellations between such large terms in the linear sigma model is tedious and for that reason modern formulations of chiral effective field theory tend to prefer a Lagrangian formulation based on a nonlinear realization of chiral symmetry [5–8]. In such a formulation the natural πNN vertex involves pseudovector (PV) coupling and the vanishing of pion-nucleon scattering amplitudes as the pion four-momentum vanishes emerges trivially. In this work, motivated by the phenomenological simplicity of enforcing soft-pion theorems, we focus on the case of PV coupling. However, since the linear realization of chiral symmetry is still used in the literature, for completeness we also compare our results with those for PS coupling.

More recently, chiral symmetry and the pion cloud of the nucleon have been shown to play a central role in understanding various flavor and spin asymmetries in quark distribution functions measured at high energies. Most prominent of these has been the SU(2) flavor asymmetry in the proton sea, with the large excess of $\bar{d}$ quarks over $\bar{u}$ being predicted in Ref. [9] and found in deep-inelastic scattering [10] and Drell-Yan experiments [11,12]. While a nonperturbative pionic component of the nucleon wave function provides a natural explanation for the sign of the observed asymmetry, calculations of the magnitude of the $\bar{d} - \bar{u}$ difference have typically been made in models without a direct connection to QCD. Furthermore, while the most convenient framework for describing high-energy reactions is the light front, the realization of chiral symmetry on the light front is yet to be fully understood (for a recent discussion see, e.g., Ref. [13]).

In Ref. [14] we examined the framework dependence of pion loop effects for the simple case of the nucleon self-energy. We showed that results for the model-independent, nonanalytical behavior associated with the long-range part of the pion cloud [15] are in fact independent of whether the calculation is performed using light front, instant form (in the rest frame or infinite momentum frame), or covariant perturbation theory. On the other hand, important differences were observed for the nonanalytic structure of the self-energy when comparing the PV and PS couplings.

Applying the methodologies developed in Refs. [14,16], we consider here the more physically relevant case of the electromagnetic coupling of the nucleon dressed by pion loops. This represents the necessary next step towards the computation of the chiral corrections to quark distribution functions of the nucleon, whose moments are given by matrix elements of twist-2 operators. The twist-2 matrix elements were studied previously by Chen and Ji [17] and Arndt and Savage [18], who computed the most important pion loop contributions to the leading nonanalytic behavior

within heavy baryon chiral perturbation theory. In the present analysis we compute the pion loop corrections to the vertex renormalization factors using a fully relativistic framework, which includes higher order corrections in the pion mass m_π. Furthermore, we demonstrate explicitly that gauge invariance and the Ward-Takahashi identities hold to all orders m_π, provided the full set of one-loop diagrams is considered, including rainbow, tadpole, and Kroll-Ruderman contact terms. We verify this for both PV and PS theories. Using the results for the vertex corrections, we then derive the pion loop corrections to the matrix elements of the twist-2 operators for both the proton and neutron, and verify the nonanalytic behavior of the isoscalar and isovector contributions. Note that for the lowest moment of the nonsinglet distribution the chiral corrections are essentially those that appear for the nucleon electromagnetic form factors at zero four-momentum transfer squared, $q^2 = 0$. These have been computed in a relativistic formalism to one loop order in Refs. [19,20]. In contrast to form factors, for high-energy observables such as quark distribution functions the natural framework is the light front, to which we specialize in this work. While we also focus on the lowest moment of the quark distributions, for the reconstruction of the distributions themselves [21], higher moments of the distributions will of course be necessary (Sec. IV).

In Sec. II we review the basics of the pion-nucleon interaction in terms of the chiral Lagrangian evaluated to lowest order in derivatives of the pion field. The electromagnetic nucleon vertex corrections arising from pion loops are computed in Sec. III, and their nonanalytic properties studied as a function of the pion mass. To illustrate the role of the various contributions to the vertex renormalization explicitly, we compute the renormalization factors numerically as a function of the ultraviolet cutoff. The results for the vertex corrections and wave function renormalization are subsequently used in Sec. IV to compute the chiral corrections to nucleon matrix elements of twist-2 operators. Comparison of the results for PV and PS coupling also allows us to identify the origin of the discrepancy between the nonanalytic behaviors of the twist-2 moments computed in heavy baryon chiral perturbation theory and at the parton level in terms of the Sullivan process [22]. Finally, in Sec. V we summarize our findings and outline future extensions of the present work. In Appendix A we collect formulas for the complete set of Feynman rules needed to compute the vertex renormalization and wave function corrections. The demonstration that the results respect gauge invariance and the Ward-Takahashi identity is presented in Appendixes B and C, respectively, and some useful results for the nonanalytic behavior of integrals are listed in Appendix D. Although some of the formal results which we summarize here can be found elsewhere, our aim will be to provide a pedagogical discussion of the derivations in order to clarify some conflicting claims in the literature about the computation of the analytic and nonanalytic contributions to the pion loop integrals.

II. PION-NUCLEON INTERACTION

To lowest order in derivatives of the pion field $\boldsymbol{\pi} = (\pi_+, \pi_-, \pi_0)$, where $\pi_\pm = (\pi_1 \mp i\pi_2)/\sqrt{2} = \pi_\mp^*$, the πNN Lagrangian is given by [5,23–25]

$$\mathcal{L}_{\pi N} = \frac{g_A}{2f_\pi}\bar{\psi}_N\gamma^\mu\gamma_5\boldsymbol{\tau}\cdot\partial_\mu\boldsymbol{\pi}\psi_N - \frac{1}{(2f_\pi)^2}\bar{\psi}_N\gamma^\mu\boldsymbol{\tau}\cdot(\boldsymbol{\pi}\times\partial_\mu\boldsymbol{\pi})\psi_N, \quad (1)$$

where ψ_N is the nucleon field, $\vec{\tau}$ is the Pauli matrix operator in nucleon isospin space, $f_\pi = 93$ MeV is the pion decay constant, and $g_A = 1.267$ is the nucleon axial vector charge. Our convention follows that in Ref. [24], but differs by an overall minus sign for the g_A term in Eq. (1) from that in Ref. [25]. For quantities where the $\boldsymbol{\pi}$ field enters quadratically, such as the pion loop corrections discussed here, the overall sign on the g_A term is immaterial. The g_A-dependent term in the Lagrangian (1) gives rise to the ''rainbow'' diagram in which a pion is emitted and absorbed by the nucleon at different space-time points, while the second is the Weinberg-Tomozawa coupling [5,26], which has two pion fields coupling to the nucleon at the same point. The latter gives the leading contribution to S-wave pion-nucleon scattering [27], and generates the pion tadpole or bubble diagrams.

The above definitions mean that the field π_- corresponds to an incoming negatively charged pion, with π_+^* to an outgoing positively charged pion. In writing Eq. (1) we have also made use of the Goldberger-Treiman relation between g_A, f_π and the πNN coupling constant $g_{\pi NN}$,

$$\frac{g_A}{f_\pi} = \frac{g_{\pi NN}}{M}, \quad (2)$$

where $g_{\pi NN} \approx 13.4$ and M is the nucleon mass.

The interaction of pions and nucleons with the electromagnetic field is introduced by minimal substitution, $\partial_\mu \to \partial_\mu + ieA_\mu$, where the charge $e = -1$ for a photon coupling to an electron. This gives rise to a $\gamma\pi N$ interaction Lagrangian of the form

$$\mathcal{L}_{\gamma\pi N} = -\bar{\psi}_N\gamma_\mu\hat{Q}_N\psi_N A_\mu + i(\partial^\mu\boldsymbol{\pi})\cdot(\hat{Q}_\pi\boldsymbol{\pi})A_\mu + \frac{ig_A}{2f_\pi}\bar{\psi}_N\gamma^\mu\gamma_5\boldsymbol{\tau}\cdot\hat{Q}_\pi\boldsymbol{\pi}\psi_N A_\mu - \frac{i}{(2f_\pi)^2}\bar{\psi}_N\gamma^\mu\boldsymbol{\tau}\cdot(\boldsymbol{\pi}\times\hat{Q}_\pi\boldsymbol{\pi})\psi_N A_\mu, \quad (3)$$

where $\hat{Q}_N = |e|(I + \tau_3)/2$ is the nucleon charge operator, defined in terms of the total isospin I of the nucleon and its

third component such that $\hat{Q}_p\psi_p = |e|\psi_p$, and $\hat{Q}_n\psi_n = 0$, and similarly for the pion charge operator one has $\hat{Q}_\pi \boldsymbol{\pi} = |e|(\pi_+, -\pi_-, 0)$. The first two terms in Eq. (3) correspond to the photon coupling to the bare nucleon and pion, respectively, the third term is the Kroll-Ruderman coupling [28,29] required by gauge invariance, while the fourth term gives rise to a photon coupling to a pion-nucleon tadpole vertex. The Lagrangians (1) and (3) can be used to derive a set of Feynman rules for computing lowest order amplitudes, which are summarized in Appendix A.

The transformation of the PS coupling Lagrangian, such as in the linear σ model [1,30], to the PV coupling Lagrangian in Eq. (1) can be understood as a canonical transformation of the field variables, analogous to the coordinate transformation from the Cartesian coordinates x and y to the plane polar coordinates $r = \sqrt{x^2 + y^2}$ and $\theta = \tan^{-1}(y/x)$ [5,31]. In analogy with the coordinate transformation, the PV coupling Lagrangian can be derived from the PS Lagrangian with the form of $x + iy$ (representing, for example, $M - g_{\pi NN}\sigma - ig_{\pi NN}\gamma_5\boldsymbol{\tau}\cdot\boldsymbol{\pi}$) by taking the equivalence between the (x, y) and (r, θ) coordinates, such that $x + iy = re^{i\theta}$ with an appropriate field redefinition for the nucleon, pion and σ fields. Since the redefined scalar field turns out to be completely decoupled after the canonical transformation and becomes irrelevant to the chiral symmetry, one may completely remove it in the PV coupling Lagrangian [5,23–25,32], as shown in Eqs. (1) and (3). In the original PS coupling Lagrangian it is crucial to keep the σ field to maintain the chiral symmetry. Thus, the pseudoscalar Lagrangian is not invariant under chiral transformations without the presence of a scalar field, as in the linear sigma model [33].

However, historically the pseudoscalar pion-nucleon interaction without a scalar field has often been discussed in the literature, with the lowest order Lagrangian density given by

$$\mathcal{L}^{\mathrm{PS}}_{\pi N} = -g_{\pi NN}\bar{\psi}_N i\gamma_5\boldsymbol{\tau}\cdot\boldsymbol{\pi}\psi_N + \cdots. \tag{4}$$

As discussed by Lensky and Pascalutsa [34], this can be formally obtained by redefining the nucleon field $\psi_N \to \xi\psi_N$, where $\xi = \exp[(ig_A\boldsymbol{\tau}\cdot\boldsymbol{\pi}/2f_\pi)\gamma_5]$, which leads to the PS Lagrangian in Eq. (4), together with the Weinberg-Tomozawa contribution in (1) replaced by an isoscalar term as in the σ model and a modified isovector term.

To contrast a number of important features pertinent to the PV and PS calculations, we discuss here the consequences of neglecting the scalar field contribution for the PS theory. For on-shell nucleons obeying the free Dirac equation, the PS and PV Lagrangians (1) give identical results for matrix elements, provided the couplings are related by Eq. (2). For off-shell nucleons, however, the PS and PV interactions lead to different results because of the strong coupling to negative energy states in the former. This can be illustrated by splitting the nucleon off-shell propagator into an on-shell part and an off-shell part, according to the identity [35]

$$\frac{1}{\not{p} - M} = \frac{\sum_s u(p,s)\bar{u}(p,s)}{p^2 - M^2} + \frac{\gamma^+}{2p^+}, \tag{5}$$

where $\gamma^+ = \gamma^0 + \gamma^3$ and $p^+ = p_0 + p_z$. One observes that while the on-shell component gives equivalent results for PV and PS interactions, the contribution from the off-shell part $\gamma^+/2p^+$ differs for the PV and PS couplings [36]. These differences were studied in detail for the case of the nucleon self-energy Σ in Ref. [14], where the leading nonanalytic behavior of Σ was found to be of order $m_\pi^2 \log m_\pi^2$ for the PS case, in contrast to the m_π^3 behavior of the PV theory. In the nucleon self-energy, the difference in the off-shell part $\gamma^+/2p^+$ indeed appears as a pion tadpole contribution in the PS theory. Since the pion tadpole involves the two-pion coupling, which corresponds to a scalar coupling, it is evident that the equivalence between the PV and PS coupling theories cannot be attained without a scalar field to restore the chiral symmetry. Important differences arise also for the vertex corrections, as we shall discuss in the following.

III. VERTEX CORRECTIONS

Beyond tree level, the interactions described by Eqs. (1) and (3) give rise to loop corrections which renormalize the electromagnetic photon–nucleon vertex. These corrections are illustrated in Fig. 1. In this section we will derive the corrections arising from each of these diagrams explicitly and study their dependence on the high-momentum cutoff mass, as well as their nonanalytic properties as a function of the pion mass. For illustration, we estimate the contribution from each diagram numerically by introducing ultraviolet regularization cutoff parameters in this work. More quantitative numerical estimates using Lorentz invariant regularization methods, such as dimensional regularization, will be presented in future work [37].

The vertex renormalization constant Z_1 is defined as

$$(Z_1^{-1} - 1)\bar{u}(p)(-i|e|\gamma^\mu)u(p) = (-i|e|)\bar{u}(p)\Lambda^\mu u(p), \tag{6}$$

where the operator Λ^μ is given by the sum of vertex correction diagrams in Figs. 1(c)–1(g), and for convenience is defined with the charge factor $(-i|e|)$ taken out. We use the convention in which the nucleon spinors are normalized according to $\bar{u}(p)u(p) = 1$. For small values of $1 - Z_1$, one also has, to lowest order in the πN coupling, $Z_1^{-1} - 1 \approx 1 - Z_1$. To evaluate the vertex renormalization constants from the various diagrams in Fig. 1, we take the $\mu = +$ components, so that

$$1 - Z_1 = \frac{M}{p^+}\bar{u}(p)\Lambda^+ u(p), \tag{7}$$

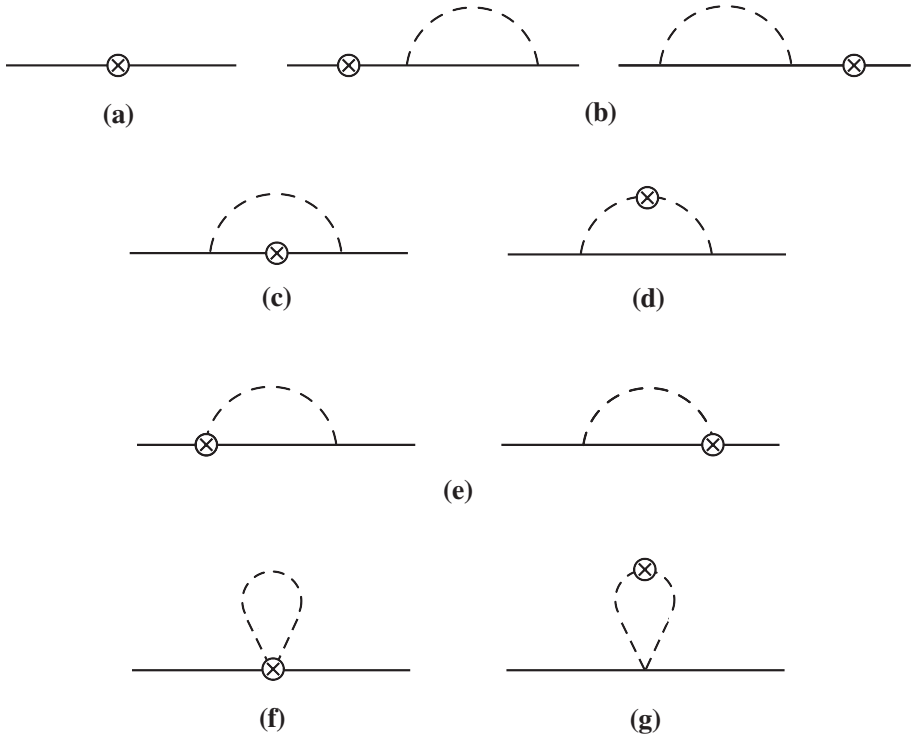

FIG. 1. Pion loop corrections to the photon–nucleon coupling in the PV pion-nucleon theory: (a) photon coupling to the bare nucleon, (b) wave function renormalization, (c) rainbow diagram with coupling to the nucleon, (d) rainbow diagram with coupling to the pion, (e) Kroll-Ruderman diagrams, (f) pion tadpole diagram with coupling to the pion-nucleon vertex, (g) pion bubble diagram with coupling to the pion.

where the $\pm$ components of the momentum four-vector are given by $p^{\pm} = p_0 \pm p_z$.

A. Photon-nucleon coupling

For the coupling of the photon to a proton dressed by a neutral π^0 loop ($p \to p + \pi^0$), Fig. 1(c), the vertex correction is computed from the operator

$$\Lambda_p^{\mu} = \left(\frac{g_A}{2f_\pi}\right)^2 \int \frac{d^4k}{(2\pi)^4} (\not{k}\gamma_5) \frac{i(\not{p} - \not{k} + M)}{D_N} \times \gamma^{\mu} \frac{i(\not{p} - \not{k} + M)}{D_N} (\gamma_5 \not{k}) \frac{i}{D_\pi}, \tag{8}$$

where we use the shorthand notation for the pion and nucleon propagators,

$$D_\pi \equiv k^2 - m_\pi^2 + i\varepsilon, \tag{9a}$$
$$D_N \equiv (p-k)^2 - M^2 + i\varepsilon, \tag{9b}$$

respectively. For a neutron target, the correction from the coupling to an intermediate state proton dressed by a negatively charged pion ($n \to p + \pi^-$) is given by $\Lambda_n^{\mu} = 2\Lambda_p^{\mu}$. Taking the $\mu = +$ component and using Eq. (7), the contribution to the vertex renormalization factor $(1 - Z_1^p) = \frac{1}{2}(1 - Z_1^n) \equiv (1 - Z_1^N)$ is then given by

$$\begin{aligned} 1 - Z_1^N &= i\left(\frac{g_A}{2f_\pi}\right)^2 \int \frac{d^4k}{(2\pi)^4} [k^4 + 4(p\cdot k)^2 - 4M^2k^2(1-y) \\ &\quad - 4p\cdot k k^2] \frac{1}{D_\pi D_N^2} \\ &= -i\left(\frac{g_A}{2f_\pi}\right)^2 \int \frac{d^4k}{(2\pi)^4} \left[\frac{4M^2(k^2 - 2yp\cdot k)}{D_\pi D_N^2} \right. \\ &\quad \left. - \frac{4M^2 y}{D_\pi D_N} - \frac{1}{D_\pi}\right], \end{aligned} \tag{10}$$

where $y = k^+/p^+$ is the fraction of the nucleon's $+$ component of momentum carried by the pion. In deriving Eq. (10) we have used the Dirac equation, $\not{p}u(p) = Mu(p)$.

Since there are two more powers of momentum k in the numerator of Z_1^N than in the denominator, the integral (10) is formally divergent. One can perform the loop integration and regularize the divergence in several ways. In Ref. [14] we considered the nucleon self-energy arising from pion dressing, and computed the loop integrals using equal-time perturbation theory in the rest frame and in the infinite momentum frame, using light-front coordinates (all with appropriate high-momentum cutoffs), and covariantly with dimensional regularization. Each method was shown to give identical results for the model-independent, nonanalytic part of the integrals, with the (model-dependent)

analytic contributions dependent upon the regularization prescription.

In the case of the vertex renormalization, it is convenient to use the + prescription to evaluate Z_1, and it will be particularly instructive to examine the integrands as a function of k^+ (or y) and $k_\perp$. Performing the k^- integration using the Cauchy integral theorem by closing the contour in the lower half-plane, one can write the nucleon contribution to the vertex renormalization as

$$1 - Z_1^N = \frac{g_A^2 M^2}{(4\pi f_\pi)^2} \int dy dk_\perp^2 \Big\{ \frac{y(k_\perp^2 + y^2 M^2)}{[k_\perp^2 + y^2 M^2 + (1-y)m_\pi^2]^2} - \frac{y}{k_\perp^2 + y^2 M^2 + (1-y)m_\pi^2} - \frac{1}{4M^2} \log\left(\frac{k_\perp^2 + m_\pi^2}{\mu^2}\right)\delta(y) \Big\}, \tag{11}$$

where the mass μ is an ultraviolet cutoff on the k^- integration. In Eq. (11) the first, second, and third terms correspond to the terms in the integrand of Eq. (10) proportional to $1/D_\pi D_N^2$, $1/D_\pi D_N$ and $1/D_\pi$, respectively. The first term, which is logarithmically divergent in $k_\perp$, gives a contribution that is equivalent to that obtained from a PS pion-nucleon coupling (4) [38,39],

$$1 - \tilde{Z}_1^N = -ig_{\pi NN}^2 \int \frac{d^4k}{(2\pi)^4} \frac{k^2 - 2yp\cdot k}{D_\pi D_N^2} = \frac{g_{\pi NN}^2}{16\pi^2} \int dy dk_\perp^2 \frac{y(k_\perp^2 + y^2 M^2)}{[k_\perp^2 + y^2 M^2 + (1-y)m_\pi^2]^2}, \tag{12}$$

where the couplings are related as in Eq. (2), and we use the tilde (" $\sim$ ") notation for quantities computed from the PS interaction. This result agrees exactly with the result from the infinite momentum frame calculation of Drell, Levy, and Yan [38] within the PS πN theory.

The second term in Eq. (11) is a new contribution, associated with the momentum dependence of the PV pion-nucleon vertex, and enters with the opposite sign to the PS-like component. The third term is nonzero only at $y = 0$, and arises from the $1/D_\pi$ term in Eq. (10). For $k_\perp \lesssim \mu$ this serves to enhance the contribution from the $1/D_\pi D_N^2$ PS-like term.

Numerically, the contributions to Z_1^N from each of the three terms are illustrated in Fig. 2 as a function of the cutoff mass Λ used to render the $k_\perp$ integration finite, taking the k^- integration cutoff $\mu = 1$ GeV. The results show large cancellation between the $1/D_\pi D_N^2$ term (which gives a negative contribution to $1 - Z_1^N$) and the $1/D_\pi D_N$ term (which gives a positive contribution), with the total closely following the residual $1/D_\pi$ contribution, which is smaller in magnitude than the other two pieces. This clearly illustrates that a calculation of the vertex renormalization using the PS πN interaction, apart from not having the correct chiral symmetry properties, yields very different results phenomenologically compared with the PV theory.

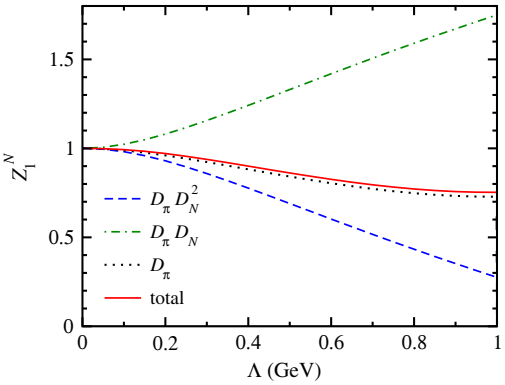

FIG. 2 (color online). Contributions to the vertex renormalization Z_1^N from terms in Eq. (10) proportional to $1/D_\pi D_N^2$ (dashed line), $1/D_\pi D_N$ (dot-dashed line), $1/D_\pi$ (dotted line), and the sum (solid line), as a function of the $k_\perp$ momentum cutoff Λ.

B. Photon-pion coupling

For the photon coupling to a positively charged pion emitted from the proton, Fig. 1(d), the corresponding operator can be written

$$\Lambda_{\pi^+}^\mu = 2\left(\frac{g_A}{2f_\pi}\right)^2 \int \frac{d^4k}{(2\pi)^4} (\not{k}\gamma_5) \frac{i(\not{p} - \not{k} + M)}{D_N} (\gamma_5 \not{k}) \times \frac{i}{D_\pi} \frac{i}{D_\pi} (2k^\mu), \tag{13}$$

where the overall isospin factor 2 accounts for the $p \to n\pi^+$ transition. For a neutron target, the operator for the coupling to the negatively charged pion in the transition $n \to p\pi^-$ would be $\Lambda_{\pi^-}^\mu = -\Lambda_{\pi^+}^\mu$. Taking the $\mu = +$ component in Eq. (13), the resulting vertex renormalization factor for the pion coupling $(1 - Z_1^{\pi^+}) = -(1 - Z_1^{\pi^-}) \equiv 2(1 - Z_1^\pi)$ can be written as

$$1 - Z_1^\pi = i\left(\frac{g_A}{2f_\pi}\right)^2 \int \frac{d^4k}{(2\pi)^4} [2(p\cdot k)^2 - k^2 p\cdot k - 2M^2 k^2] \times \frac{2y}{D_\pi^2 D_N} = -i\left(\frac{g_A}{2f_\pi}\right)^2 \int \frac{d^4k}{(2\pi)^4} \Big[\frac{8yM^2 p\cdot k}{D_\pi^2 D_N} + \frac{2yp\cdot k}{D_\pi^2} + \frac{4yM^2}{D_\pi^2} \Big], \tag{14}$$

where Z_1^π here is defined with the isospin factor removed. Because y is odd in k^+, while D_π^2 is even, the third term in Eq. (14) proportional to y/D_π^2 will vanish after integration over k^+. For the second term, proportional to $2yp\cdot k/D_\pi^2$, we can use the identity

$$\int d^4k \frac{2yp\cdot k}{D_\pi^2} = \int d^4k \frac{1}{D_\pi}. \tag{15}$$

In fact, since

$$\frac{\partial}{\partial k^+}\frac{1}{D_\pi^n} = -\frac{nk^-}{D_\pi^{n+1}}, \tag{16}$$

one has, for any integer n,

$$\int d^4k \frac{2yp\cdot k}{D_\pi^{n+1}} = \frac{1}{n}\int d^4k \frac{1}{D_\pi^n}. \tag{17}$$

Using the relation (15), and performing the k^- integration by closing the contour in the upper half-plane, the photon–pion coupling contribution to Z_1 can be written as

$$1 - Z_1^\pi = \frac{g_A^2 M^2}{(4\pi f_\pi)^2}\int dy dk_\perp^2 \Big\{\frac{y(k_\perp^2 + y^2M^2)}{[k_\perp^2 + y^2M^2 + (1-y)m_\pi^2]^2} + \frac{1}{4M^2}\log\Big(\frac{k_\perp^2 + m_\pi^2}{\mu^2}\Big)\delta(y)\Big\}. \tag{18}$$

Note that the first term in Eq. (18) is identical to the first term in Eq. (11) for the Z_1^p contribution to the vertex renormalization. It is also the result one obtains from the "Sullivan process" [9,22,40–45] for the contribution of the pion cloud to the deep-inelastic structure function of the nucleon, where the current couples to the pion cloud, leaving an on-shell nucleon in the final state. These analyses all utilized the PS pion-nucleon interaction, in which the vertex renormalization factor is given by

$$1 - \tilde{Z}_1^\pi = -ig_{\pi NN}^2 \int \frac{d^4k}{(2\pi)^4}\frac{2yp\cdot k}{D_\pi^2 D_N} = \frac{g_{\pi NN}^2}{16\pi^2}\int dy dk_\perp^2 \frac{y(k_\perp^2 + y^2M^2)}{[k_\perp^2 + y^2M^2 + (1-y)m_\pi^2]^2}. \tag{19}$$

This result also coincides with the vertex renormalization computed in the infinite momentum frame in Ref. [38] in terms of nucleon and pion "partons" in the PS theory. Comparison of Eqs. (19) and (12) also demonstrates that the PS model respects the charge conservation condition,

$$1 - \tilde{Z}_1^\pi = 1 - \tilde{Z}_1^N, \tag{20}$$

which follows directly from the Ward-Takahashi identity (see Appendix C).

In contrast, the full PV result for Z_1^π in Eq. (18) contains in addition a singular, δ function term in y, just as in Eq. (11) for Z_1^p but with the opposite sign. As illustrated in Fig. 3, this term cancels some of the contribution from the PS, $1/D_\pi D_N^2$ term, leaving an overall positive contribution to $1 - Z_1^\pi$. Clearly the PV Z_1^π and Z_1^p results are different for any value of the $k_\perp$ cutoff Λ, and in order to demonstrate their equivalence requires consideration of additional terms arising from the derivative PV coupling.

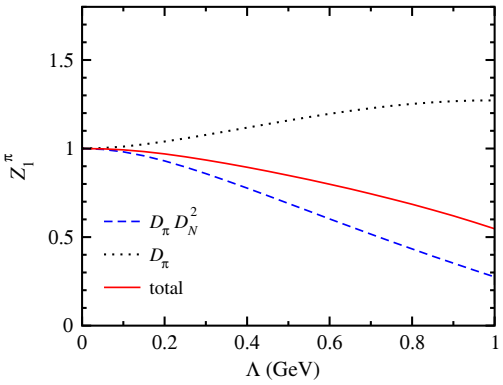

FIG. 3 (color online). Contributions to the vertex renormalization Z_1^π from terms in Eq. (18) proportional to $1/D_\pi D_N$ (dot-dashed line), $1/D_\pi$ (dotted line), and the sum (solid line), as a function of the $k_\perp$ momentum cutoff Λ.

C. Kroll-Ruderman terms

The momentum dependence of the PV πN interaction gives rise to an additional Kroll-Ruderman (KR) term [26] which describes the photon coupling to the πNN vertex, Fig. 1(e). For the case of the $p \to n\pi^+$ vertex, these are computed from the operator

$$\Lambda^\mu_{\mathrm{KR},\pi^+} = 2i\Big(\frac{g_A}{2f_\pi}\Big)^2 \int \frac{d^4k}{(2\pi)^4}\Big(\not{k}\gamma_5 \frac{i(\not{p} - \not{k} + M)}{D_N}\gamma^\mu\gamma_5 + \gamma_5\gamma^\mu \frac{i(\not{p} - \not{k} + M)}{D_N}\gamma_5\not{k}\Big)\frac{i}{D_\pi}. \tag{21}$$

For a neutron target, the corresponding operator describing the photon coupling to the $n \to p\pi^-$ vertex is $\Lambda^\mu_{\mathrm{KR},\pi^-} = -\Lambda^\mu_{\mathrm{KR},\pi^+}$. Note that the emission of a neutron π^0 does not give rise to a KR correction term.

The contribution to the vertex renormalization factor is then given by $(1 - Z_1^{\mathrm{KR},\pi^+}) = -(1 - Z_1^{\mathrm{KR},\pi^-}) \equiv 2(1 - Z_1^{\mathrm{KR}})$, where

$$1 - Z_1^{\mathrm{KR}} = -i\Big(\frac{g_A}{2f_\pi}\Big)^2 \int \frac{d^4k}{(2\pi)^4}(2k^2 - 4p\cdot k + 4M^2 y) \times \frac{1}{D_\pi D_N} = -i\Big(\frac{g_A}{2f_\pi}\Big)^2 \int \frac{d^4k}{(2\pi)^4}\Big(-\frac{4M^2 y}{D_\pi D_N} - \frac{2}{D_\pi}\Big). \tag{22}$$

Performing the k^- integration, the resulting contribution to $1 - Z_1$ is

$$1 - Z_1^{\mathrm{KR}} = -\frac{g_A^2 M^2}{(4\pi f_\pi)^2}\int dy dk_\perp^2 \Big\{\frac{y}{k_\perp^2 + y^2M^2 + (1-y)m_\pi^2} + \frac{1}{2M^2}\log\Big(\frac{k_\perp^2 + m_\pi^2}{\mu^2}\Big)\delta(y)\Big\}, \tag{23}$$

where the first term in the integrand arises from the $1/D_\pi D_N$ term, while the $\delta(y)$ term is associated with the $1/D_\pi$ contribution in Eq. (22).

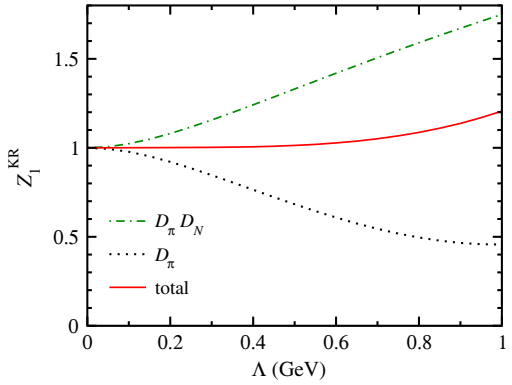

FIG. 4 (color online). Contributions to the vertex renormalization Z_1^{KR} from terms in Eq. (23) proportional to $1/D_\pi D_N$ (dot-dashed line), $1/D_\pi$ (dotted line), and the sum (solid line), as a function of the $k_\perp$ momentum cutoff Λ.

The contributions from the individual terms to Z_1^{KR} are shown in Fig. 4 as a function of the $k_\perp$ momentum cutoff Λ, as well as the total KR correction. Note the large cancellation between the $1/D_\pi$ and $1/D_\pi D_N$ terms for values of the cutoff $\Lambda \lesssim 0.8$ GeV. Omission of the δ-function $1/D_\pi$ contribution would thus lead to a significant overestimate of the KR correction.

Formally, the Kroll-Ruderman terms are needed to ensure gauge invariance in the PV theory. Indeed, from Eqs. (11), (18), and (23) one can verify explicitly that

$$(1 - Z_1^N) = (1 - Z_1^\pi) + (1 - Z_1^{\mathrm{KR}}) \tag{24}$$

for the PV case. In contrast, in the PS theory, where the πN vertex is independent of momentum, there is no analogous KR contribution, and gauge invariance is reflected through the relation (20). In Fig. 5 we show the total contributions to Z_1 from the nucleon and pion rainbow diagrams, Z_1^N and Z_1^π, and the total KR correction. The sum of these three terms is of course zero by Eq. (24).

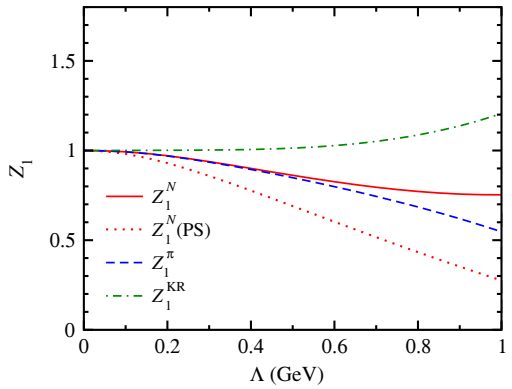

FIG. 5 (color online). Contributions to the vertex renormalization Z_1 from the photon–nucleon coupling Z_1^N (solid line), photon–pion coupling Z_1^π (dashed line), and Kroll-Ruderman terms Z_1^{KR} (dot-dashed line), as a function of the $k_\perp$ momentum cutoff Λ. Note that the sum of the pion tadpole and bubble contributions to Z_1 vanishes.

D. Tadpoles and bubbles

At lowest order the Lagrangian (3) contains, in addition to the PV coupling of the pion to the nucleon, quadratic terms arising from the covariant derivative. For the coupling of the photon to the $\pi\pi pp$ vertex in the pion tadpole diagram in Fig. 1(f) the relevant operator is

$$\Lambda^\mu_{p\mathrm{tad}} = -\frac{1}{2f_\pi^2}\int \frac{d^4k}{(2\pi)^4}\gamma^\mu \frac{i}{D_\pi}. \tag{25}$$

For the coupling to the $\pi\pi nn$ vertex, the corresponding operator is $\Lambda^\mu_{n\mathrm{tad}} = -\Lambda^\mu_{p\mathrm{tad}}$. The contribution to the vertex renormalization from the $\pi\pi NN$ tadpoles is then $(1 - Z_1^{N\mathrm{tad}}) \equiv (1 - Z_1^{p\mathrm{tad}}) = -(1 - Z_1^{n\mathrm{tad}})$, where

$$1 - Z_1^{N\mathrm{tad}} = -\frac{i}{2f_\pi^2}\int \frac{d^4k}{(2\pi)^4}\frac{1}{D_\pi}. \tag{26}$$

After integration over k^-, this can be written

$$1 - Z_1^{N\mathrm{tad}} = \frac{1}{2(4\pi f_\pi)^2}\int dy dk_\perp^2 \log\left(\frac{k_\perp^2 + m_\pi^2}{\mu^2}\right)\delta(y). \tag{27}$$

For the bubble diagram with the photon coupling directly to a pion, Fig. 1(g), the relevant operator for a proton target is

$$\Lambda^\mu_{\pi\mathrm{bub}(p)} = \frac{1}{2f_\pi^2}\int \frac{d^4k}{(2\pi)^4}(-i\not{k})2k^\mu \frac{i}{D_\pi}\frac{i}{D_\pi}, \tag{28}$$

with that for a neutron target given by $\Lambda^\mu_{\pi\mathrm{bub}(n)} = -\Lambda^\mu_{\pi\mathrm{bub}(p)}$. Taking the $\mu = +$ component on both sides of Eq. (28), the contribution to the vertex renormalization is given by $(1 - Z_1^{\pi\mathrm{bub}}) \equiv (1 - Z_1^{\pi\mathrm{bub}(p)}) = -(1 - Z_1^{\pi\mathrm{bub}(n)})$, where

$$1 - Z_1^{\pi\mathrm{bub}} = \frac{i}{2f_\pi^2}\int \frac{d^4k}{(2\pi)^4}\frac{2yp\cdot k}{D_\pi^2}. \tag{29}$$

Using the identify (15) this can be written, after k^- integration, as

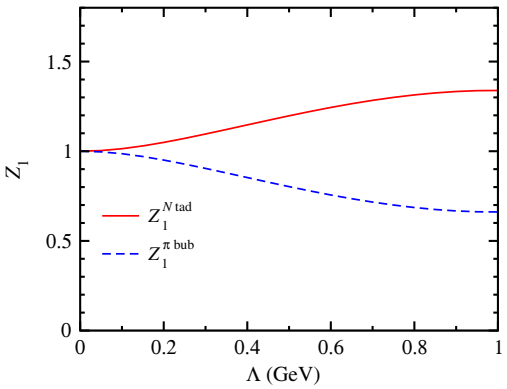

FIG. 6 (color online). Nucleon tadpole (solid line) and pion bubble (dashed line) contributions to the vertex renormalization as a function of the $k_\perp$ momentum cutoff Λ.

$$1 - Z_1^{\pi\text{bub}} = -\frac{1}{2(4\pi f_\pi)^2}\int dy dk_\perp^2 \log\left(\frac{k_\perp^2 + m_\pi^2}{\mu^2}\right)\delta(y), \tag{30}$$

which is equal and opposite to the pion tadpole contribution in Eq. (27). The vanishing of the sum of the pion tadpole and bubble contributions,

$$(1 - Z_1^{\pi\text{bub}}) + (1 - Z_1^{N\text{tad}}) = 0, \tag{31}$$

ensures therefore that these have no net effect on the vertex renormalization. In Fig. 6 the pion tadpole and bubble diagrams are illustrated for a $k_\perp$ momentum cutoff Λ.

E. Nonanalytic behavior

The model-independent, nonanalytic (NA) structure of the vertex renormalization factors can be studied by expanding $1 - Z_1$ in powers of m_π. The terms in the expansion that are even powers of m_π are analytic in the quark mass m_q (from the Gell-Mann–Oakes–Renner relation, $m_\pi^2 \sim m_q$ for small m_π), while odd powers of m_π or logarithms of m_π are nonanalytic in m_q. The NA terms reflect the long-range structure of chiral loops, and are exactly calculable in terms of low-energy constants such as g_A and f_π, independent of the details of short-range physics.

The NA behavior of the nucleon rainbow contribution is given by

$$\begin{aligned}(1 - Z_1^N) \overset{\text{NA}}{\to} \frac{g_A^2 M^2}{(4\pi f_\pi)^2}\Bigg\{&\frac{m_\pi^2}{M^2}\log m_\pi^2 - \frac{5\pi}{4}\frac{m_\pi^3}{M^3} - \frac{3m_\pi^4}{4M^4}\log m_\pi^2 && \left[\frac{1}{D_\pi D_N^2}\text{term}\right]\\ &- \frac{m_\pi^2}{2M^2}\log m_\pi^2 + \frac{\pi}{2}\frac{m_\pi^3}{M^3} + \frac{m_\pi^4}{4M^4}\log m_\pi^2 && \left[\frac{1}{D_\pi D_N}\text{term}\right]\\ &+ \frac{m_\pi^2}{4M^2}\log m_\pi^2\Bigg\} && \left[\frac{1}{D_\pi}\text{term}\right]\\ = \frac{3g_A^2}{4(4\pi f_\pi)^2}&\left\{m_\pi^2\log m_\pi^2 - \pi\frac{m_\pi^3}{M} - \frac{2m_\pi^4}{3M^2}\log m_\pi^2 + \mathcal{O}(m_\pi^5)\right\},\end{aligned} \tag{32}$$

where for completeness we have included the first three lowest order NA terms, and the origins of the various powers of m_π have been indicated in the brackets to the right of the equations. Comparison with the PS result [the $1/D_\pi D_N^2$ term in Eq. (32)] shows that for the leading NA (LNA) term (order $m_\pi^2 \log m_\pi^2$) one has

$$(1 - Z_1^N)_{\text{LNA}} = \frac{3}{4}(1 - \tilde{Z}_1^N)_{\text{LNA}}. \tag{33}$$

This makes clear the origin of the difference between the results in Refs. [38,39], which were obtained for a PS πN coupling, and Refs. [17,18], which were obtained for the PV theory. Note that this result does not depend on the details of the ultraviolet regulator, since the nonanalytic structure is determined entirely by the infrared behavior of the integrals.

The NA behavior of the pion rainbow contribution is given, to order in m_π, by

$$\begin{aligned}(1 - Z_1^\pi) \overset{\text{NA}}{\to} \frac{g_A^2 M^2}{(4\pi f_\pi)^2}\Bigg\{&\frac{m_\pi^2}{M^2}\log m_\pi^2 - \frac{5\pi}{4}\frac{m_\pi^3}{M^3} - \frac{3m_\pi^4}{4M^4}\log m_\pi^2 && \left[\frac{1}{D_\pi^2 D_N}\text{ term}\right]\\ &- \frac{m_\pi^2}{4M^2}\log m_\pi^2\Bigg\} && \left[\frac{1}{D_\pi}\text{ term}\right]\\ = \frac{3g_A^2}{4(4\pi f_\pi)^2}&\left\{m_\pi^2\log m_\pi^2 - \frac{5\pi}{3}\frac{m_\pi^3}{M} - \frac{m_\pi^4}{M^2}\log m_\pi^2 + \mathcal{O}(m_\pi^5)\right\}.\end{aligned} \tag{34}$$

Note that the behavior arising from the $1/D_\pi^2 D_N$ term is identical to that from the $1/D_\pi D_N^2$ term in Z_1^N, which reflects the gauge invariance of the PS theory, Eq. (20).

For the PV theory, the Kroll-Ruderman terms has the nonanalytic behavior

$$\begin{aligned}(1 - Z_1^{\text{KR}}) \overset{\text{NA}}{\to} \frac{g_A^2 M^2}{(4\pi f_\pi)^2}\Bigg\{&-\frac{m_\pi^2}{2M^2}\log m_\pi^2 + \frac{\pi}{2}\frac{m_\pi^3}{M^3} + \frac{m_\pi^4}{4M^4}\log m_\pi^2 && \left[\frac{1}{D_\pi D_N}\text{term}\right]\\ &+ \frac{m_\pi^2}{2M^2}\log m_\pi^2\Bigg\} && \left[\frac{1}{D_\pi}\text{term}\right]\\ = \frac{3g_A^2}{4(4\pi f_\pi)^2}&\left\{\frac{2\pi}{3}\frac{m_\pi^3}{M} - \frac{m_\pi^4}{3M^2}\log m_\pi^2 + \mathcal{O}(m_\pi^5)\right\}.\end{aligned} \tag{35}$$

TABLE I. Leading nonanalytic contributions to the vertex renormalization $1 - Z_1$, in units of $1/(4\pi f_\pi)^2 m_\pi^2 \log m_\pi^2$. The asterisks (*) in the Z_1^N and Z_1^π rows denote contributions that are present for the pseudoscalar πN coupling. Note that the nonanalytic contributions from the KR terms cancel at this order, but are nonzero at $\mathcal{O}(m_\pi^3)$, and are needed to ensure gauge invariance of the theory, Eq. (24). The sum of all contributions is given in the last two columns for the PV and PS theories, respectively.

	$1/D_\pi D_N^2$	$1/D_\pi^2 D_N$	$1/D_\pi D_N$	$1/D_\pi$ or $1/D_\pi^2$	Sum (PV)	Sum (PS)
$1 - Z_1^N$	g_A^{2*}	0	$-\frac{1}{2} g_A^2$	$\frac{1}{4} g_A^2$	$\frac{3}{4} g_A^2$	g_A^2
$1 - Z_1^\pi$	0	g_A^{2*}	0	$-\frac{1}{4} g_A^2$	$\frac{3}{4} g_A^2$	g_A^2
$1 - Z_1^{\rm KR}$	0	0	$-\frac{1}{2} g_A^2$	$\frac{1}{2} g_A^2$	0	0
$1 - Z_1^{N\rm tad}$	0	0	0	$-1/2$	$-1/2$	0
$1 - Z_1^{\pi\rm bub}$	0	0	0	$1/2$	$1/2$	0

Here the $\mathcal{O}(m_\pi^2 \log m_\pi^2)$ terms cancel between the $1/D_\pi D_N$ and $1/D_\pi$ terms, so that the leading NA behavior of the KR term $\sim m_\pi^3$. For the sum of the Z_1^π and $Z_1^{\rm KR}$ terms,

$$(1 - Z_1^\pi) + (1 - Z_1^{\rm KR}) \xrightarrow{\rm NA} \frac{3 g_A^2}{4(4\pi f_\pi)^2} \left\{ m_\pi^2 \log m_\pi^2 - \pi \frac{m_\pi^3}{M} - \frac{2 m_\pi^4}{3 M^2} \log m_\pi^2 \right\}, \quad (36)$$

the NA behavior is therefore explicitly verified to be equivalent to that in $(1 - Z_1^N)$ in Eq. (32).

Finally, for the pion loop contributions from Sec. III D, the NA behavior is given by the $m_\pi^2 \log m_\pi^2$ term for both the pion tadpole [Fig. 1(f)] and bubble [Fig. 1(g)] diagrams,

$$(1 - Z_1^{N\rm tad}) \xrightarrow{\rm NA} -\frac{1}{2(4\pi f_\pi)^2} m_\pi^2 \log m_\pi^2, \quad (37)$$

$$(1 - Z_1^{\pi\rm bub}) \xrightarrow{\rm NA} \frac{1}{2(4\pi f_\pi)^2} m_\pi^2 \log m_\pi^2. \quad (38)$$

The results for the leading order nonanalytic contributions to the vertex renormalization factors are summarized in Table I for each of the above terms, where the entries are given in units of $1/(4\pi f_\pi)^2 m_\pi^2 \log m_\pi^2$. Note that the contributions from the terms associated with $1/D_\pi D_N^2$ and $1/D_\pi^2 D_N$ (denoted by asterisks *) are the same as those in the PS theory, while the other contributions arise only for PV coupling. The table clearly illustrates the origin of the difference between the $1 - Z_1^N$ corrections in the PV and PS theories, and in particular the relative factor 3/4 found in heavy baryon chiral perturbation theory [17,18] compared with calculations based on the Sullivan process with PS coupling [22,38].

IV. PARTON DISTRIBUTIONS AND MOMENTS

The above results on the vertex renormalization factors can be used to compute the NA behavior of moments of parton distribution functions (PDFs) arising from the pion cloud of the nucleon. The presence of the pion cloud induces corrections to the PDFs of a bare nucleon, whose Bjorken x dependence can be represented in terms of convolutions of pion and nucleon light-cone distribution functions $f_i(y)$ and the corresponding parton distributions in the pion and nucleon [16]. The light-cone distribution $f_i(y)$ are defined such that when integrated over y they give the appropriate vertex renormalization factors Z_1^i, $(1 - Z_1^i) = \int dy f_i(y)$. Unlike in the PS coupling models [9,22,40–46], the dressed nucleon PDFs in the PV theory contain several additional terms [16,47],

$$q(x) = Z_2 q_0(x) + ([f_N + f_{N\rm tad}] \otimes q_0)(x) + ([f_\pi + f_{\pi\rm bub}] \otimes q_\pi)(x) + (f_{\rm KR} \otimes q_{\rm KR})(x), \quad (39)$$

where q_0 is the bare nucleon PDF [arising from the diagram in Fig. 1(a)], q_π is the PDF in the pion, and $q_{\rm KR} \equiv \Delta q_0 / g_A$, with Δq_0 the spin-dependent PDF in the bare nucleon. The constant Z_2 is the wave function renormalization constant, and the symbol $\otimes$ represents the convolution integral $(f \otimes q)(x) = \int_x^1 (dz/z) f(z) q(x/z)$, where for the f_π and $f_{\pi\rm bub}$ contributions the integration variable z should be taken to be the fraction of the nucleon's + component of momentum carried by the pion, $y = k^+/p^+$, while for the f_N, $f_{N\rm tad}$, and $f_{\rm KR}$ terms $z = 1 - y$. Note that because of the additional pion field at the vertex in the KR diagram, Fig. 1(e), the contribution of the KR terms to the (unpolarized) PDF involves a convolution with a spin-dependent parton distribution. In the corresponding "Sullivan" process based on the PS coupling [9,22,40–44], only the f_N and f_π functions contribute, and these are related by Eq. (20).

A. Pionic corrections to twist-2 matrix elements

According to the operator product expansion in QCD, the moments of PDFs are related to matrix elements of local operators,

$$\langle N | \hat{\mathcal{O}}_q^{\mu_1 \cdots \mu_n} | N \rangle = 2 \langle x^{n-1} \rangle_q p^{\{\mu_1} \cdots p^{\mu_n\}}, \quad (40)$$

where the braces $\{\cdots\}$ denote symmetrization of Lorentz indices, and the operators are given by the quark bilinears

$$\hat{\mathcal{O}}_q^{\mu_1\cdots\mu_n} = \bar{\psi}\gamma^{\{\mu_1} iD^{\mu_2}\ldots iD^{\mu_n\}}\psi - \text{traces}, \quad (41)$$

with D^μ the covariant derivative. The nth moment of the PDF $q(x)$ is given by

$$\langle x^{n-1}\rangle_q = \int_0^1 dx x^{n-1}(q(x) + (-1)^n\bar{q}(x)). \quad (42)$$

For $n = 1$, we define $\langle x^0\rangle_q \equiv \mathcal{M}^{(p)}$ to be the moment in the proton, with $u \leftrightarrow d$ for the neutron $\mathcal{M}^{(n)}$.

For the direct coupling of the photon to the nucleon, which includes the wave function renormalization [Fig. 1(b)], the nucleon rainbow diagram [Fig. 1(c)], and the pion tadpole diagram [Fig. 1(f)], the contributions to the twist-2 matrix elements are given by

$$\mathcal{M}_N^{(p)} = Z_2 + (1 - Z_1^N) + (1 - Z_1^{N\text{tad}}), \quad (43a)$$
$$\mathcal{M}_N^{(n)} = 2(1 - Z_1^N) - (1 - Z_1^{N\text{tad}}), \quad (43b)$$

for the proton and neutron, respectively. The wave function renormalization Z_2 factor in Eq. (43a) is

$$1 - Z_2 = (1 - Z_1^p) + (1 - Z_1^n) = 3(1 - Z_1^N). \quad (44)$$

The contributions from the photon–pion couplings, including the pion rainbow diagram [Fig. 1(d)], the Kroll-Ruderman term [Fig. 1(e)], and the pion bubble diagram [Fig. 1(g)], are given for the proton and neutron by

$$\mathcal{M}_\pi^{(p)} = 2(1 - Z_1^\pi) + 2(1 - Z_1^{\text{KR}}) + (1 - Z_1^{\pi\text{bub}}), \quad (45a)$$
$$\mathcal{M}_\pi^{(n)} = -2(1 - Z_1^\pi) - 2(1 - Z_1^{\text{KR}}) - (1 - Z_1^{\pi\text{bub}}). \quad (45b)$$

Using Eq. (44), the pion cloud contributions to the isoscalar (sum of proton and neutron) moments from coupling involving nucleons cancel,

$$\mathcal{M}_N^{(p+n)} = 1, \quad (46)$$

leaving the charge of the nucleon (or valence quark number) unrenormalized from that given by the bare coupling, Fig. 1(a). Similarly, the contributions to the isoscalar moments involving direct coupling to pions add to zero, as required by charge conservation,

$$\mathcal{M}_\pi^{(p+n)} = 0. \quad (47)$$

Note that these results, Eqs. (46) and (47), are true to all orders in the pion mass, not just for the LNA parts that were discussed in Refs. [17,18,48], and to which we turn to in the next section.

B. LNA behavior of isovector moments

The LNA contributions from the nucleon coupling diagrams to the proton and neutron moments are given by

$$\mathcal{M}_N^{(p)} \xrightarrow{\text{LNA}} 1 - \frac{(3g_A^2 + 1)}{2(4\pi f_\pi)^2} m_\pi^2 \log m_\pi^2, \quad (48a)$$
$$\mathcal{M}_N^{(n)} \xrightarrow{\text{LNA}} \frac{(3g_A^2 + 1)}{2(4\pi f_\pi)^2} m_\pi^2 \log m_\pi^2. \quad (48b)$$

Taking the difference between the proton and neutron moments, the isovector contribution then becomes

$$\mathcal{M}_N^{(p-n)} \xrightarrow{\text{LNA}} 1 - \frac{(3g_A^2 + 1)}{(4\pi f_\pi)^2} m_\pi^2 \log m_\pi^2, \quad (49)$$

which agrees with the results obtained in heavy baryon chiral perturbation theory [17,18].

Similarly, the LNA contributions from the pion coupling diagrams to the proton and neutron moments are given by

$$\mathcal{M}_\pi^{(p)} \xrightarrow{\text{LNA}} \frac{(3g_A^2 + 1)}{2(4\pi f_\pi)^2} m_\pi^2 \log m_\pi^2, \quad (50a)$$
$$\mathcal{M}_\pi^{(n)} \xrightarrow{\text{LNA}} -\frac{(3g_A^2 + 1)}{2(4\pi f_\pi)^2} m_\pi^2 \log m_\pi^2, \quad (50b)$$

so that the isovector contribution can be written

$$\mathcal{M}_\pi^{(p-n)} \xrightarrow{\text{LNA}} \frac{(3g_A^2 + 1)}{(4\pi f_\pi)^2} m_\pi^2 \log m_\pi^2. \quad (51)$$

The pion coupling contributions to the moment therefore cancel those of the nucleon coupling in Eq. (49), such that the total lowest moment of the PDF is not affected by pion loop corrections.

The analysis is more straightforward for the PS theory, where neither tadpoles, bubbles nor KR terms are present, and LNA behavior of the nucleon and pion coupling contributions to the isovector moments is given by

$$\tilde{\mathcal{M}}_N^{(p-n)} \xrightarrow{\text{LNA}} 1 - \frac{4g_A^2}{(4\pi f_\pi)^2} m_\pi^2 \log m_\pi^2, \quad (52a)$$
$$\tilde{\mathcal{M}}_\pi^{(p-n)} \xrightarrow{\text{LNA}} \frac{4g_A^2}{(4\pi f_\pi)^2} m_\pi^2 \log m_\pi^2. \quad (52b)$$

This agrees with the results obtained in Ref. [39] using the light-cone momentum distributions computed for the Sullivan process in the PS theory [22,38]. As observed in Ref. [17], the PV and PS results agree in the limit as $g_A \to 1$, although they clearly differ in the general case for $g_A \neq 1$.

For higher moments, $n > 1$, the pion coupling contributions will be suppressed by additional powers of m_π^2, while the LNA behavior of the nucleon coupling diagrams remains $\sim m_\pi^2 \log m_\pi^2$ [17,18,48]. Cancellation will therefore not occur between the nucleon and pion coupling contributions for these moments, so that the shape of underlying PDFs will in general be modified by the presence of pion loops. We have verified that our LNA results agree with those presented in Ref. [47]. Further details of the pion light-cone momentum distribution $f_i(y)$ are discussed in Ref. [16], and an analysis of their phenomenological

consequences will be presented in a forthcoming publication [37].

V. CONCLUSION

In this work we have presented a detailed analysis of pion cloud corrections to the electromagnetic coupling of the nucleon, using the lowest order effective Lagrangian constrained by the chiral symmetry of QCD. We have computed the complete set of vertex corrections arising from the various one-loop diagrams, including rainbow diagrams with pion and nucleon coupling, Kroll-Ruderman contributions, and tadpole and bubble diagrams associated with πN contact interactions.

Explicit evaluation of the vertex renormalization factors allowed us to directly verify relations between the nucleon and pion coupling diagrams, and demonstrate the consistency of the theory with electromagnetic gauge invariance. The KR terms in particular are essential for ensuring gauge invariance to all orders in the pion mass, even though these do not contribute to the leading nonanalytic behavior of the vertex factors. We have also shown that the sum of the pion tadpole and bubble diagrams vanishes.

We have examined the chiral expansion of all the vertex corrections as a function of the pion mass m_π, computing the coefficients of the nonanalytic terms up to and including order $m_\pi^4 \log m_\pi$. The LNA terms agree with earlier calculations in heavy baryon chiral perturbation theory [17,18], although our formulation is relativistic and allows for higher order corrections in m_π/M. Comparison of the results for the pseudoscalar πN theory reveals the origin of the longstanding discrepancy between the LNA behavior in the chiral effective theory and in approaches based on the Sullivan process [22,38,44,45] which use a γ_5 coupling.

To study the behavior of the total vertex corrections, rather than just their longest-range LNA contributions, we have computed the vertex renormalization factors numerically as a function of the transverse momentum cutoff used to regularize the integrals. The pion and nucleon rainbow corrections give positive contributions to the vertex renormalization factor $(1 - Z_1)$ for the range of cutoffs considered here ($\Lambda \leq 1$ GeV), while the contribution from the KR diagram is negative. The overall magnitude of the vertex correction is $(1 - Z_1^N) = (1 - Z_1^\pi) + (1 - Z_1^{\mathrm{KR}}) \approx 15\%$ for $\Lambda = 0.5$ GeV and $\approx 25\%$ for $\Lambda = 1$ GeV. The tadpole and bubble contributions range up to $\approx 30\%$ for $\Lambda = 1$ GeV. Although a transverse momentum cutoff breaks the Lorentz invariance of the πN theory, for the purposes of the present study it is sufficient to illustrate the relative contributions of the various pion loop diagrams. For a more quantitative analysis, for example, of the corrections to the $\bar{d} - \bar{u}$ PDF difference, a covariant regularization scheme can be used [37].

Finally, using the results for the vertex and wave function renormalization constants we computed the pion loop corrections to the matrix elements of twist-2 operators for the proton and neutron, which in the operator product expansion are related to moments of parton distribution functions. For the lowest moment, we demonstrated explicitly that the pion loop corrections cancel for the isoscalar combination of moments for the nucleon and pion couplings separately. The isovector moments, on the other hand, were found to have the characteristic $m_\pi^2 \log m_\pi^2$ leading dependence for both the nucleon and pion coupling diagrams (with the sum of course canceling, as required by charge conservation). Again, comparison of the PV and PS results for the moments enabled us to clearly identify the source of the difference between the coefficients of the LNA terms in the two theories. While the PV theory is clearly preferred by considerations of chiral symmetry, the explicit demonstration that the PS theory can be made consistent in this context with the introduction of a scalar σ field remains an interesting challenge.

The results derived here can be used in the future to investigate the nonanalytic behavior of the nucleon PDFs, particularly the extrapolation of calculations in lattice QCD performed at unphysically large quark masses [49,50] to the physical region. Our findings will also pave the way for phenomenological studies, especially the quest for a consistent interpretation of the physics of the pion cloud at the parton level, enabling deeper studies of the origin of the $\bar{d} - \bar{u}$ asymmetry [16]. In addition, this work will also guide investigation of the very important asymmetry between the s and $\bar{s}$ distributions, with its connection to the five-quark component of the nucleon wave function, as well as the spin-flavor asymmetry $\Delta\bar{u} - \Delta\bar{d}$ between the polarized $\bar{u}$ and $\bar{d}$ distributions.

ACKNOWLEDGMENTS

We thank M. Birse, M. Burkardt, K. Hendricks, V. Lyubovitskij, M. Polyakov, and A. A. Vladimirov for helpful discussions. This work was supported by the DOE Contract No. DE-AC05-06OR23177, under which Jefferson Science Associates, LLC operates Jefferson Lab, DOE Contract No. DE-FG02-03ER41260, and the Australian Research Council through the ARC Centre of Excellence for Particle Physics at the Terascale and Grant FL0992247.

APPENDIX A: FEYNMAN RULES

For convenience we summarize in this appendix the complete set of Feynman rules derived from the PV Lagrangian $\mathcal{L}_{\gamma\pi N}$ in Eq. (3), needed to compute the vertex renormalization and wave function corrections from pion loops. The conventions throughout this work denote the nucleon momentum by p^μ and the pion momentum by k^μ, with e the electric charge on the electron. Isospin couplings that are not listed are identically zero.

Propagators

Nucleon: $\frac{i}{\not{p} - M}$ (A1)

Pion: $\frac{i}{k^2 - m_\pi^2}$ (A2)

γ^*NN vertex

$\gamma^* p\,(n) \to p\,(n)$: 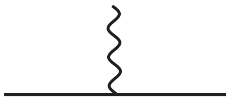 $-iQ_{p(n)}\,|e|\,\gamma^\mu$ with $Q_{p(n)} = 1\,(0)$ (A3)

$\gamma^*\pi\pi$ vertex

$\gamma^*\pi^\pm \to \pi^\pm$: 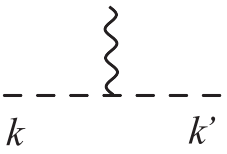 $-iQ_{\pi^\pm}\,|e|\,(k + k')^\mu$ with $Q_{\pi^\pm} = \pm 1$ (A4)

πNN vertex

$p\,(n) \to \pi^0\,p\,(n)$: 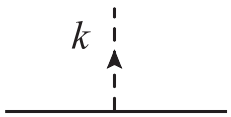 $+1\,(-1)\,\frac{g_A}{2f_\pi}\gamma_5 \not{k}$ (A5)

$p\,(n) \to \pi^+(\pi^-)\,n\,(p)$: $\frac{g_A}{\sqrt{2}f_\pi}\gamma_5 \not{k}$ (A6)

$\gamma^*\pi$NN vertex

$\gamma^* p\,(n) \to \pi^+(\pi^-)\,n\,(p)$:  $-1(+1)\frac{g_A|e|}{\sqrt{2}f_\pi}\gamma_5\,\gamma^\mu$ (A7)

$\pi\pi$NN vertex

$\pi^-(\pi^+)\,p \to \pi^-(\pi^+)\,p$: $+1(-1)\frac{i}{4f_\pi^2}(\not{k} + \not{k}')$ (A8)

$\pi^-(\pi^+)\,n \to \pi^-(\pi^+)\,n$:  $-1(+1)\frac{i}{4f_\pi^2}(\not{k} + \not{k}')$ (A9)

$\pi^0\,p\,(n) \to \pi^+(\pi^-)\,n\,(p)$: $+1(-1)\frac{i}{2\sqrt{2}f_\pi^2}(\not{k} + \not{k}')$ (A10)

$\gamma^*\pi\pi$NN vertex

$\pi^\pm\,p\,(n) \to \pi^\pm\,p\,(n)$: 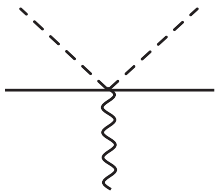 $+1(-1)\frac{i|e|}{2f_\pi^2}\gamma^\mu$ (A11)

$\pi^0\,p\,(n) \to \pi^+(\pi^-)\,n\,(p)$: $-\frac{i|e|}{2\sqrt{2}f_\pi^2}\gamma^\mu$ (A12)

APPENDIX B: GAUGE INVARIANCE

In this section we demonstrate explicitly that the electromagnetic coupling to the nucleon dressed by pions, illustrated in Fig. 7, is gauge invariant, for both the PV and PS pion-nucleon theories.

For the $\pi^0 pp$ coupling the current derived from the PV Lagrangian in Eq. (3) is a sum of the three contributions in Figs. 7(a)–7(c),

$$J^\mu_{(\pi^0)} = \frac{g_A^2}{4f_\pi^2}\int \frac{d^4k}{(2\pi)^4}[\mathcal{J}^\mu_{\rm wf(L)} + \mathcal{J}^\mu_{\rm wf(R)} + \mathcal{J}^\mu_N], \tag{B1}$$

where

$$\mathcal{J}^\mu_{\rm wf(L)} = \bar u(p+q)\not k\gamma_5 \frac{i}{\not p+\not q-\not k-M}\gamma_5\not k\frac{i}{\not p+\not q-M} \times(-ie\gamma^\mu)u(p)\frac{i}{D_\pi(k)}, \tag{B2a}$$

$$\mathcal{J}^\mu_{\rm wf(R)} = \bar u(p+q)(-ie\gamma^\mu)\frac{i}{\not p-M}\not k\gamma_5\frac{i}{\not p-\not k-M} \times\gamma_5\not k u(p)\frac{i}{D_\pi(k)}, \tag{B2b}$$

represent the "wave function renormalization" diagrams in Figs. 7(a) and 7(b), and

$$\mathcal{J}^\mu_N = \bar u(p+q)\not k\gamma_5\frac{i}{\not p+\not q-\not k-M}(-ie\gamma^\mu) \times\frac{i}{\not p-\not k-M}\gamma_5\not k u(p)\frac{i}{D_\pi(k)} \tag{B3}$$

corresponds to the rainbow diagram with coupling to the proton in Fig. 7(c). Here the electromagnetic current operator brings in a finite momentum q to the proton. Contracting the currents with the photon four-vector q_μ and using the Dirac equation $(\not p - M)u(p) = 0$, one finds

$$q_\mu\mathcal{J}^\mu_{\rm wf(L)} = e\bar u(p+q)\gamma_5\not k\frac{1}{\not p+\not q-\not k-M}\gamma_5\not k u(p)\frac{1}{D_\pi(k)}, \tag{B4a}$$

$$q_\mu\mathcal{J}^\mu_{\rm wf(R)} = -e\bar u(p+q)\gamma_5\not k\frac{1}{\not p-\not k-M}\gamma_5\not k u(p)\frac{1}{D_\pi(k)}, \tag{B4b}$$

and

$$q_\mu\mathcal{J}^\mu_N = e\bar u(p+q)\gamma_5\not k\left(\frac{1}{\not p-\not k-M}-\frac{1}{\not p+\not q-\not k-M}\right) \times\gamma_5\not k u(p)\frac{1}{D_\pi(k)} = -q_\mu\mathcal{J}^\mu_{\rm wf(L)} - q_\mu\mathcal{J}^\mu_{\rm wf(R)}, \tag{B4c}$$

where we have used $\not q = (\not p+\not q-M)-(\not p-M)$ and $\not q = (\not p+\not q-\not k-M)-(\not p-\not k-M)$ to simplify Eqs. (B4b) and (B4c), respectively. The sum of the three contributions then gives the required result,

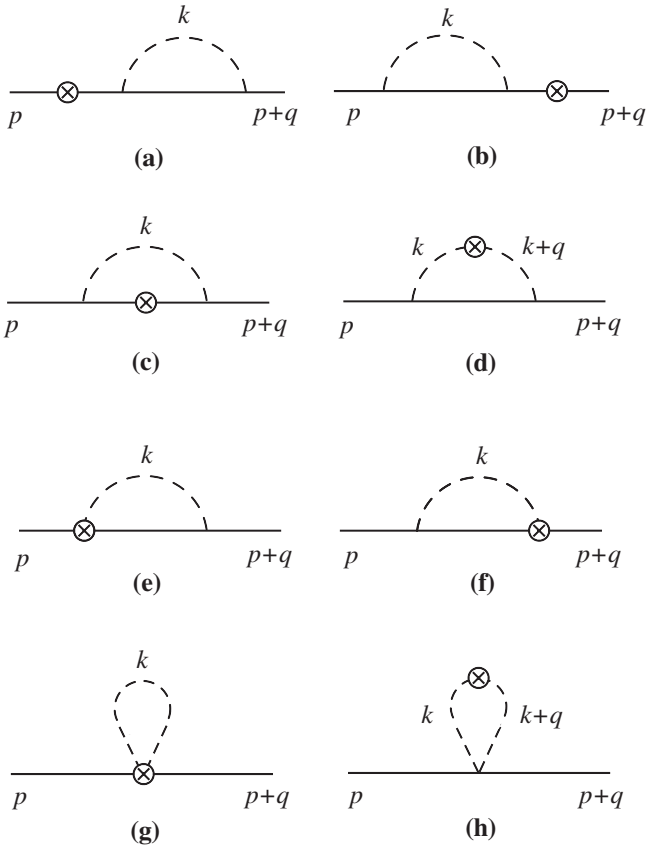

FIG. 7. Coupling of an electromagnetic current to a proton (with momentum p) dressed by a pion (with momentum k): (a), (b) wave function renormalization diagrams, (c) rainbow diagram with coupling to the proton, (d) rainbow diagram with coupling to the π^+, (e), (f) Kroll-Ruderman diagrams, (g) tadpole diagram with coupling to the $\pi\pi pp$ vertex, (h) bubble diagram with coupling to the pion. The current brings in a momentum q.

$$q_\mu J^\mu_{(\pi^0)} = 0. \tag{B5}$$

For the $\pi^+ np$ coupling the current has seven contributions, including the wave function renormalization diagrams in Figs. 7(a) and 7(b), the π^+ rainbow diagram in Fig. 7(d), the Kroll-Ruderman contributions in Figs. 7(e) and 7(f), and the π^+ tadpoles and bubbles in Figs. 7(g) and 7(h),

$$J^\mu_{(\pi^+)} = \int\frac{d^4k}{(2\pi)^4}\left\{\frac{g_A^2}{2f_\pi^2}[\mathcal{J}^\mu_{\rm wf(L)} + \mathcal{J}^\mu_{\rm wf(R)} + \mathcal{J}^\mu_\pi + \mathcal{J}^\mu_{\rm KR(L)} + \mathcal{J}^\mu_{\rm KR(R)}] + \frac{1}{4f_\pi^2}[\mathcal{J}^\mu_{N\rm tad} + \mathcal{J}^\mu_{\pi\rm bub}]\right\}. \tag{B6}$$

The current for the π^+ rainbow is given by

$$\mathcal{J}^\mu_\pi = \bar u(p+q)(\not k+\not q)\gamma_5\frac{i}{\not p-\not k-M}\gamma_5\not k u(p) \times\frac{i}{D_\pi(k+q)}(-ie)(2k^\mu+q^\mu)\frac{i}{D_\pi(k)}, \tag{B7}$$

while the Kroll-Ruderman currents are

$$\mathcal{J}^{\mu}_{\mathrm{KR(L)}} = \bar{u}(p+q)\not{k}\gamma_5 \frac{i}{\not{p}+\not{q}-\not{k}-M}(-e\gamma_5\gamma^{\mu})u(p)\frac{i}{D_{\pi}(k)}, \tag{B8a}$$

$$\mathcal{J}^{\mu}_{\mathrm{KR(R)}} = \bar{u}(p+q)(e\gamma_5\gamma^{\mu})\frac{i}{\not{p}-\not{k}-M}\gamma_5\not{k}u(p)\frac{i}{D_{\pi}(k)}. \tag{B8b}$$

Finally, for the pion tadpole and bubble diagrams the two currents are given by

$$\mathcal{J}^{\mu}_{N\mathrm{tad}} = -i\bar{u}(p+q)(2\not{k}+\not{q})u(p)(-ie)(2k^{\mu}+q^{\mu})\frac{i}{D_{\pi}(k)}\frac{i}{D_{\pi}(k+q)}, \tag{B9a}$$

$$\mathcal{J}^{\mu}_{\pi\mathrm{bub}} = 2i\bar{u}(p+q)e\gamma^{\mu}u(p)\frac{i}{D_{\pi}(k)}, \tag{B9b}$$

respectively. Note that diagrams involving a pion tadpole with the photon coupling to a proton in the initial or final state directly involve loop integrations with an odd number of factors k in the integrand [see Eq. (A8)] and therefore vanish identically.

Contracting the π^+ currents with the photon momentum q_{μ}, one has

$$q_{\mu}\mathcal{J}^{\mu}_{\pi} = e\bar{u}(p+q)\gamma_5(\not{k}+\not{q})\frac{1}{\not{p}-\not{k}-M}\gamma_5\not{k}u(p)\left(\frac{1}{D_{\pi}(k)}-\frac{1}{D_{\pi}(k+q)}\right), \tag{B10a}$$

$$q_{\mu}\mathcal{J}^{\mu}_{\mathrm{KR(L)}} = -e\bar{u}(p+q)\gamma_5\not{k}\frac{1}{\not{p}+\not{q}-\not{k}-M}\gamma_5\not{q}u(p)\frac{1}{D_{\pi}(k)}, \tag{B10b}$$

$$q_{\mu}\mathcal{J}^{\mu}_{\mathrm{KR(R)}} = -e\bar{u}(p+q)\gamma_5\not{q}\frac{1}{\not{p}-\not{k}-M}\gamma_5\not{k}u(p)\frac{1}{D_{\pi}(k)}. \tag{B10c}$$

Adding the wave function renormalization contributions in Eqs. (B4a) and (B4b), one can verify, after some tedious but straightforward manipulations, that

$$q_{\mu}J^{\mu}_{(\pi^+)} = 0. \tag{B11}$$

Note that the inclusion of the KR contributions is vital to cancel the contributions from the π^+ current with the PV coupling, without which the theory would not be gauge invariant. The tadpole and bubble contributions are each independently gauge invariant, as can be seen from the contractions

$$q_{\mu}\mathcal{J}^{\mu}_{N\mathrm{tad}} = e\bar{u}(p+q)(2\not{k}+\not{q})u(p)\left(\frac{1}{D_{\pi}(k)}-\frac{1}{D_{\pi}(k+q)}\right) = 0, \tag{B12a}$$

$$q_{\mu}\mathcal{J}^{\mu}_{\pi\mathrm{bub}} = -2e\bar{u}(p+q)\not{q}u(p)\frac{i}{D_{\pi}(k)} = 0, \tag{B12b}$$

where the first expression can be verified by changing variables $\not{k}' = \not{k}+\not{q} \to \not{k}$, and the second vanishes because of the Dirac equation. The same of course holds true also for a neutron initial state.

For the PS coupling, only the diagrams in Figs. 7(a)–7(d) are present. As in the PV case, for the $\pi^0 pp$ coupling the current in the PS theory has three contributions from Figs. 7(a)–7(c),

$$\tilde{J}^{\mu}_{(\pi^0)} = g^2_{\pi NN}\int\frac{d^4k}{(2\pi)^4}[\tilde{\mathcal{J}}^{\mu}_{\mathrm{wf(L)}} + \tilde{\mathcal{J}}^{\mu}_{\mathrm{wf(R)}} + \tilde{\mathcal{J}}^{\mu}_{N}], \tag{B13}$$

where

$$\tilde{\mathcal{J}}^{\mu}_{\mathrm{wf(L)}} = \bar{u}(p+q)i\gamma_5\frac{i}{\not{p}+\not{q}-\not{k}-M}i\gamma_5\frac{i}{\not{p}+\not{q}-M}(-ie\gamma^{\mu})u(p)\frac{i}{D_{\pi}(k)}, \tag{B14a}$$

$$\tilde{\mathcal{J}}^{\mu}_{\mathrm{wf(R)}} = \bar{u}(p+q)(-ie\gamma^{\mu})\frac{i}{\not{p}-M}i\gamma_5\frac{i}{\not{p}-\not{k}-M}i\gamma_5 u(p)\frac{i}{D_{\pi}(k)}, \tag{B14b}$$

$$\tilde{\mathcal{J}}^{\mu}_{N} = \bar{u}(p+q)i\gamma_5\frac{i}{\not{p}+\not{q}-\not{k}-M}(-ie\gamma^{\mu})\frac{i}{\not{p}-\not{k}-M}i\gamma_5 u(p)\frac{i}{D_{\pi}(k)}. \tag{B14c}$$

Contracting the currents (B14) with q_{μ} and again using the Dirac equation, one finds

$$q_\mu \tilde{\mathcal{J}}^\mu_{\mathrm{wf(L)}} = e\bar{u}(p+q)\gamma_5 \frac{1}{\not p + \not q - \not k - M}\gamma_5 u(p)\frac{1}{D_\pi(k)}, \tag{B15a}$$

$$q_\mu \tilde{\mathcal{J}}^\mu_{\mathrm{wf(R)}} = -e\bar{u}(p+q)\gamma_5 \frac{1}{\not p - \not k - M}\gamma_5 u(p)\frac{1}{D_\pi(k)}, \tag{B15b}$$

$$q_\mu \tilde{\mathcal{J}}^\mu_{N} = e\bar{u}(p+q)\gamma_5\left(\frac{1}{\not p - \not k - M} - \frac{1}{\not p + \not q - \not k - M}\right)\gamma_5 u(p)\frac{1}{D_\pi(k)}. \tag{B15c}$$

From Eqs. (B15) it is evident that

$$q_\mu \tilde{\mathcal{J}}^\mu_{N} = -q_\mu \tilde{\mathcal{J}}^\mu_{\mathrm{wf(L)}} - q_\mu \tilde{\mathcal{J}}^\mu_{\mathrm{wf(R)}}, \tag{B16}$$

so that gauge invariance is satisfied explicitly for the proton dressed by a neutral π^0 with PS coupling,

$$q_\mu \tilde{J}^\mu_{(\pi^0)} = 0. \tag{B17}$$

Similarly for the PS $\pi^+ np$ coupling, the current is given by the three contributions in Figs. 7(a), 7(b), and 7(d),

$$\tilde{J}^{\,\mu}_{(\pi^+)} = 2g^2_{\pi NN}\int \frac{d^4k}{(2\pi)^4}[\tilde{\mathcal{J}}^\mu_{\mathrm{wf(L)}} + \tilde{\mathcal{J}}^\mu_{\mathrm{wf(R)}} + \tilde{\mathcal{J}}^\mu_{\pi}], \tag{B18}$$

where

$$\tilde{\mathcal{J}}^\mu_{\pi} = \bar{u}(p+q)i\gamma_5 \frac{i}{\not p - \not k - M} i\gamma_5 u(p) \times \frac{i}{D_\pi(k+q)}(-ie)(2k^\mu + q^\mu)\frac{i}{D_\pi(k)}. \tag{B19}$$

The contraction of q_μ with $\tilde{\mathcal{J}}^\mu_\pi$ gives

$$q_\mu \tilde{\mathcal{J}}^\mu_{\pi} = e\bar{u}(p+q)\gamma_5 \frac{i}{\not p - \not k - M}\gamma_5 \times\left(\frac{1}{D_\pi(k)} - \frac{1}{D_\pi(k+q)}\right), \tag{B20}$$

where the first term in the parentheses cancels with $q_\mu \tilde{\mathcal{J}}^\mu_{\mathrm{wf(R)}}$ in Eq. (B15b), and the second cancels with $q_\mu \tilde{\mathcal{J}}^\mu_{\mathrm{wf(L)}}$ in (B15a) after changing variables $\not k' = \not k + \not q \to \not k$. Therefore gauge invariance is explicitly verified also for the π^+ with PS coupling,

$$q_\mu \tilde{J}^\mu_{(\pi^+)} = 0. \tag{B21}$$

Note that since these results are obtained at the operator level, they are independent of the particular renormaliation scheme chosen to regulate the integrals.

APPENDIX C: WARD-TAKAHASHI IDENTITY

In this section we demonstrate the consistency of the vertex corrections and wave function renormalization with the Ward-Takahashi identity. To begin with, we consider the nucleon self-energy operator, which can in general be written in terms of the vector and scalar components as

$$\hat{\Sigma}(p) = \Sigma_v \not p + \Sigma_s. \tag{C1}$$

Evaluating the matrix element of the self-energy operator between on-shell nucleon states gives

$$\Sigma = \frac{1}{2}\sum_s \bar{u}(p,s)\hat{\Sigma}(p)u(p,s) = M\Sigma_v + \Sigma_s, \tag{C2}$$

where the sum is taken over the spin polarizations $s = \pm 1/2$ of the nucleon. The self-energy modifies the pole of the nucleon propagator according to

$$\frac{1}{\not p - M - \hat{\Sigma}(p)} = \frac{Z_2}{\not p - M - \delta M}, \tag{C3}$$

where Z_2 is the wave function renormalization constant,

$$Z_2 = \frac{1}{1-\Sigma_v}, \tag{C4}$$

and the mass shift δM is given by

$$\delta M = Z_2\Sigma. \tag{C5}$$

Alternatively, using Eqs. (C4) and (C5) one can express the vector and scalar components of the self-energy as

$$\Sigma_v = -(Z_2^{-1} - 1), \tag{C6}$$

$$\Sigma_s = (Z_2^{-1} - 1)M + Z_2^{-1}\delta M. \tag{C7}$$

From Eqs. (C1) and (C6) one observes that the nucleon wave function renormalization Z_2 is related to the derivative of the nucleon self-energy operator by

$$(Z_2 - 1)\gamma^\mu = \frac{\partial \hat{\Sigma}(p)}{\partial p_\mu}. \tag{C8}$$

On the other hand, from Eq. (6) in Sec. III the vertex renormalization constant Z_1 is defined in terms of the matrix element of the vertex correction Λ^μ by

$$(Z_1^{-1} - 1)\bar{u}(p)\gamma^\mu u(p) = \bar{u}(p)\Lambda^\mu u(p). \tag{C9}$$

The Ward-Takahashi identity relates the vertex operator Λ^μ to the p_μ derivative of the self-energy operator $\hat{\Sigma}$, which can be expressed as the equality of the vertex and wave function renormalization factors, $Z_1 = Z_2$.

To demonstrate that this relation is explicitly satisfied by the PV pion-nucleon theory defined by Eqs. (1) and (3), recall that the self-energy for a nucleon dressed by a pion loop is given by [14]

$$\hat{\Sigma}(p) = 3i\left(\frac{g_A}{2f_\pi}\right)^2 \int \frac{d^4k}{(2\pi)^4} (\not{k}\gamma_5) \frac{i(\not{p} - \not{k} + M)}{D_N(p-k)} (\gamma_5 \not{k}) \frac{i}{D_\pi(k)}, \tag{C10}$$

where $D_N(p-k) = (p-k)^2 - M^2 + i\varepsilon$ and $D_\pi(k) = k^2 - m_\pi^2 + i\varepsilon$. Differentiating the nucleon propagator with respect to the nucleon momentum, which is equivalent to the insertion of a zero energy photon,

$$\frac{\partial}{\partial p_\mu} \frac{1}{\not{p} - \not{k} - M} = -\frac{1}{\not{p} - \not{k} - M} \gamma^\mu \frac{1}{\not{p} - \not{k} - M}, \tag{C11}$$

leads to

$$-\frac{\partial \hat{\Sigma}(p)}{\partial p_\mu} = 3\left(\frac{g_A}{2f_\pi}\right)^2 \int \frac{d^4k}{(2\pi)^4} (\not{k}\gamma_5) \frac{i(\not{p} - \not{k} + M)}{D_N(p-k)} \times \gamma^\mu \frac{i(\not{p} - \not{k} + M)}{D_N(p-k)} (\gamma_5 \not{k}) \frac{i}{D_\pi(k)}. \tag{C12}$$

Comparing the right-hand side of (C12) with the expression for Λ^μ in Eq. (8), one can then identify

$$3\Lambda_p^\mu = -\frac{\partial \hat{\Sigma}(p)}{\partial p_\mu}. \tag{C13}$$

Now, changing variables $k \to p - k$ in Eq. (C10) enables the self-energy to be written equivalently as

$$\hat{\Sigma}(p) = 3i\left(\frac{g_A}{2f_\pi}\right)^2 \int \frac{d^4k}{(2\pi)^4} (\not{p} - \not{k}) \times \gamma_5 \frac{i(\not{k} + M)}{D_N(k)} \gamma_5 (\not{p} - \not{k}) \frac{i}{D_\pi(p-k)}, \tag{C14}$$

which when differentiated with respect to p_μ gives rise to three terms,

$$-\frac{\partial \hat{\Sigma}(p)}{\partial p_\mu} = 3\left(\frac{g_A}{2f_\pi}\right)^2 \int \frac{d^4k}{(2\pi)^4} \left\{ 2(p-k)^\mu (\not{p} - \not{k}) \gamma_5 \frac{i(\not{k} + M)}{D_N(k)} \gamma_5 (\not{p} - \not{k}) \left(\frac{i}{D_\pi(p-k)}\right)^2 - i\gamma^\mu \gamma_5 \frac{i(\not{k} + M)}{D_N(k)} \gamma_5 (\not{p} - \not{k}) \frac{i}{D_\pi(p-k)} - (\not{p} - \not{k}) \gamma_5 \frac{i(\not{k} + M)}{D_N(k)} i\gamma_5 \gamma^\mu \frac{i}{D_\pi(p-k)} \right\}. \tag{C15a}$$

Changing variables $k \to p - k$ once again then gives

$$3\frac{1}{2}\left(\Lambda^\mu_{\pi^+} + \Lambda^\mu_{\mathrm{KR},\pi^+}\right) = -\frac{\partial \hat{\Sigma}(p)}{\partial p_\mu}. \tag{C15b}$$

Since the expressions for $\hat{\Sigma}(p)$ in Eqs. (C10) and (C14) are equivalent, this implies that the electromagnetic operators are related by

$$\Lambda_p^\mu = \frac{1}{2}(\Lambda^\mu_{\pi^+} + \Lambda^\mu_{\mathrm{KR},\pi^+}). \tag{C16}$$

Taking matrix elements of both sides of Eq. (C16) between proton states, one arrives at the relation

$$(1 - Z_1^p) = \frac{1}{2}(1 - Z_1^{\pi^+}) + \frac{1}{2}(1 - Z_1^{\mathrm{KR},\pi^+}), \tag{C17}$$

or, in terms of the "isoscalar" vertex factors defined in Sec. III, the desired expression $(1 - Z_1^N) = (1 - Z_1^\pi) + (1 - Z_1^{\mathrm{KR}})$ as in Eq. (24).

The proof for the PS case follows similarly, and is in fact more straightforward since the KR terms are absent in this case. One can also check the validity of the Ward-Takahashi identity by performing the integrations explicitly, and comparing the integrated expressions for the vertex renormalization factors.

APPENDIX D: NONANALYTIC BEHAVIOR OF INTEGRALS

In this appendix we summarize some useful results for the integrals appearing in the expressions for the vertex corrections in Sec. III and the self-energies Appendix C, using dimensional regularization to render ultraviolet divergent integrals finite. Expanding the results in powers of m_π, we also provide explicit expressions for their nonanalytic behavior in the chiral limit.

For the integrals involving only the pion propagator $(1/D_\pi)$,

$$\int d^4k \frac{1}{D_\pi} = i\pi^2 m_\pi^2 \left[\frac{1}{\varepsilon} + 1 - \gamma - \log\pi - \log\frac{m_\pi^2}{\mu^2} + \mathcal{O}(\varepsilon)\right] \overset{\mathrm{NA}}{\to} - i\pi^2 m_\pi^2 \log m_\pi^2, \tag{D1}$$

$$\int d^4k \frac{1}{D_\pi^2} = i\pi^2 \left[\frac{1}{\varepsilon} - \gamma - \log\pi - \log\frac{m_\pi^2}{\mu^2} + \mathcal{O}(\varepsilon)\right] \overset{\mathrm{NA}}{\to} - i\pi^2 \log m_\pi^2. \tag{D2}$$

The expressions in Eqs. (D1) and (D2) can also be related using

$$\frac{\partial}{\partial m_\pi^2}\int d^4k\frac{1}{D_\pi}=\int d^4k\frac{1}{D_\pi^2}. \tag{D3}$$

Note that there are no higher order contributions in m_π for either of these integrals. The corresponding integrals involving only the nucleon propagator $(1/D_N)$, on the other hand, do not have nonanalytic contributions,

$$\int d^4k\frac{1}{D_N}=i\pi^2M^2\left[\frac{1}{\varepsilon}+1-\gamma-\log\pi-\log\frac{M^2}{\mu^2}+\mathcal{O}(\varepsilon)\right]\overset{\text{NA}}{\to}0, \tag{D4}$$

$$\int d^4k\frac{1}{D_N^2}=i\pi^2\left[\frac{1}{\varepsilon}-\gamma-\log\pi-\log\frac{M^2}{\mu^2}+\mathcal{O}(\varepsilon)\right]\overset{\text{NA}}{\to}0. \tag{D5}$$

For the integral of one pion propagator and one nucleon propagator, one has

$$\begin{aligned}\int d^4k\frac{1}{D_\pi D_N}&=i\pi^2\left[\frac{1}{\varepsilon}+2-\gamma-\log\pi-\log\frac{M^2}{\mu^2}-\frac{m_\pi^2}{2M^2}\log\frac{m_\pi^2}{M^2}-\frac{m_\pi r}{M^2}\left(\tan^{-1}\frac{m_\pi}{r}+\tan^{-1}\frac{2M^2-m_\pi^2}{m_\pi r}\right)\right]\\&\overset{\text{NA}}{\to}-\frac{i\pi^2}{2M^2}[m_\pi^2\log m_\pi^2+2\pi Mm_\pi+\mathcal{O}(m_\pi^3)],\end{aligned} \tag{D6}$$

where $r=\sqrt{4M^2-m_\pi^2}$. Note that this term is responsible for the leading $\mathcal{O}(m_\pi^3)$ behavior of the nucleon self-energy [14].

Finally, for integrals involving one pion and two nucleon propagators, or one nucleon and two pion propagators, the additional powers of the loop momentum render the results finite,

$$\begin{aligned}\int d^4k\frac{1}{D_\pi^2D_N}&=-i\pi^2\frac{1}{M^2}\left[\frac{1}{2}\log\frac{m_\pi^2}{M^2}-\frac{m_\pi^2-2M^2}{m_\pi r}\left(\tan^{-1}\frac{m_\pi}{r}+\tan^{-1}\frac{2M^2-m_\pi^2}{m_\pi r}\right)\right]\\&\overset{\text{NA}}{\to}-\frac{i\pi^2}{2M^2}\left[\log m_\pi^2+\frac{\pi M}{m_\pi}+\mathcal{O}(m_\pi)\right],\end{aligned} \tag{D7}$$

$$\begin{aligned}\int d^4k\frac{1}{D_\pi D_N^2}&=i\pi^2\frac{1}{M^2}\left[\frac{1}{2}\log\frac{m_\pi^2}{M^2}-\frac{m_\pi}{r}\left(\tan^{-1}\frac{m_\pi}{r}+\tan^{-1}\frac{2M^2-m_\pi^2}{m_\pi r}\right)\right]\\&\overset{\text{NA}}{\to}\frac{i\pi^2}{2M^2}\left[\log m_\pi^2-\frac{\pi m_\pi}{2M}+\mathcal{O}(m_\pi^3)\right].\end{aligned} \tag{D8}$$

The expressions in Eqs. (D6) and (D7) can also be related using

$$\frac{\partial}{\partial m_\pi^2}\int d^4k\frac{1}{D_\pi D_N}=\int d^4k\frac{1}{D_\pi^2D_N}. \tag{D9}$$

[1] M. Gell-Mann and M. Levy, Nuovo Cimento **16**, 705 (1960).
[2] M. Gell-Mann, Phys. Rev. **125**, 1067 (1962).
[3] Y. Nambu and E. Schrauner, Phys. Rev. **128**, 862 (1962).
[4] S. L. Adler, Phys. Rev. **143**, 1144 (1966).
[5] S. Weinberg, Phys. Rev. Lett. **18**, 188 (1967).
[6] H. Pagels, Phys. Rep. **16**, 219 (1975).
[7] S. Weinberg, Physica (Amsterdam) **96**, 327 (1979).
[8] J. Gasser and H. Leutwyler, Ann. Phys. (N.Y.) **158**, 142 (1984).
[9] A. W. Thomas, Phys. Lett. **126B**, 97 (1983).
[10] P. Amaudraz *et al.*, Phys. Rev. Lett. **66**, 2712 (1991); M. Arneodo *et al.*, Phys. Lett. B **364**, 107 (1995).
[11] A. Baldit *et al.*, Phys. Lett. B **332**, 244 (1994).
[12] E. A. Hawker *et al.*, Phys. Rev. Lett. **80**, 3715 (1998).
[13] S. R. Beane, Ann. Phys. (N.Y.) **337**, 111 (2013).
[14] C.-R. Ji, W. Melnitchouk, and A. W. Thomas, Phys. Rev. D **80**, 054018 (2009).
[15] L.-F. Li and H. Pagels, Phys. Rev. Lett. **26**, 1204 (1971).
[16] M. Burkardt, K. S. Hendricks, C.-R. Ji, W. Melnitchouk, and A. W. Thomas, Phys. Rev. D **87**, 056009 (2013).
[17] J.-W. Chen and X. Ji, Phys. Lett. B **523**, 107 (2001).
[18] D. Arndt and M. J. Savage, Nucl. Phys. **A697**, 429 (2002).
[19] B. Kubis and U.-G. Meissner, Nucl. Phys. **A679**, 698 (2001).
[20] T. Fuchs, J. Gegelia, and S. Scherer, J. Phys. G **30**, 1407 (2004).
[21] W. Detmold, W. Melnitchouk, and A. W. Thomas, Eur. Phys. J. direct C **3**, 1 (2001).
[22] J. D. Sullivan, Phys. Rev. D **5**, 1732 (1972).

[23] A. Krause, Helv. Phys. Acta **63**, 3 (1990).
[24] E. E. Jenkins and A. V. Manohar, Phys. Lett. B **255**, 558 (1991).
[25] V. Bernard, N. Kaiser, and U. G. Meissner, Int. J. Mod. Phys. E **04**, 193 (1995).
[26] Y. Tomozawa, Nuovo Cimento A **46**, 707 (1966).
[27] S. Weinberg, Phys. Rev. Lett. **17**, 616 (1966).
[28] N. M. Kroll and M. A. Ruderman, Phys. Rev. **93**, 233 (1954).
[29] D. Drechsel and L. Tiator, J. Phys. G **18**, 449 (1992).
[30] J. S. Schwinger, Ann. Phys. (N.Y.) **2**, 407 (1957).
[31] J. D. Walecka, *Theoretical Nuclear and Subnuclear Physics* (Oxford University Press, New York, 1995).
[32] A. W. Thomas, J. Phys. G **7**, L283 (1981).
[33] A. W. Thomas and W. Weise, *The Structure of the Nucleon* (Wiley-VCH, Berlin, 2001).
[34] V. Lensky and V. Pascalutsa, Pis'ma Zh. Eksp. Teor. Fiz. **89**, 127 (2009) [JETP Lett. **89**, 108 (2009)].
[35] S.-J. Chang and T.-M. Yan, Phys. Rev. D **7**, 1147 (1973).
[36] C.-R. Ji, W. Melnitchouk, and A. W. Thomas, Phys. Rev. Lett. **110**, 179101 (2013).
[37] C.-R. Ji *et al.* (work in progress).
[38] S. D. Drell, D. J. Levy, and T. M. Yan, Phys. Rev. D **1**, 1035 (1970).
[39] A. W. Thomas, W. Melnitchouk, and F. M. Steffens, Phys. Rev. Lett. **85**, 2892 (2000).
[40] E. M. Henley and G. A. Miller, Phys. Lett. B **251**, 453 (1990).
[41] V. R. Zoller, Z. Phys. C **53**, 443 (1992).
[42] W. Melnitchouk and A. W. Thomas, Phys. Rev. D **47**, 3794 (1993).
[43] H. Holtmann, A. Szczurek, and J. Speth, Nucl. Phys. **A596**, 631 (1996).
[44] J. Speth and A. W. Thomas, Adv. Nucl. Phys. **24**, 83 (2002).
[45] S. Kumano, Phys. Rep. **303**, 183 (1998).
[46] M. Alberg and G. A. Miller, Phys. Rev. Lett. **108**, 172001 (2012).
[47] A. M. Moiseeva and A. A. Vladimirov, Eur. Phys. J. A **49**, 23 (2013).
[48] J.-W. Chen and X. Ji, Phys. Rev. Lett. **87**, 152002 (2001); **88**, 249901(E) (2002).
[49] W. Detmold, W. Melnitchouk, J. W. Negele, D. B. Renner, and A. W. Thomas, Phys. Rev. Lett. **87**, 172001 (2001).
[50] G. S. Bali, S. Collins, M. Deka, B. Gläßle, M. Göckeler, J. Najjar, A. Nobile, D. Pleiter, A. Schäfer, and A. Sternbeck, Phys. Rev. D **86**, 054504 (2012).